NTNU

Norwegian University of Science and Technology

Faculty of Information Technology, Mathematics and Electrical Engineering

Department of Engineering Cybernetics

MSC THESIS DESCRIPTION SHEET

Name: Johan Fredrik Holm Totland

Department: Engineering Cybernetics

Thesis Title: Fast Pressure Control in Managed Pressure Drilling

Background

In drilling operations performed in the oil and gas industry it is important to control pressure in the well. Drilling fluid, also called mud, is pumped into the well at a constant rate, and pressure in the well is controlled by a choke at the top of the well (in Managed Pressure Drilling). The control objective is to keep the pressure at the bottom of the well close to a given set-point. In the project work last fall, a model of the pressure and flow in the well was developed based on discretization of a distributed parameter model. The model facilitates efficient controller design, yet is detailed enough to capture the dominant dynamics within a desired closed-loop bandwidth.

The goal of the present work is to design control algorithms based on the model, which achieve faster pressure control than what is possible with conventional control. The following points should be addressed by the student:

Tasks:

1. Review current practices for pressure control in MPD.
2. Review modeling from the project work. Revise the model, if necessary.
3. Suggest a model based control design procedure for fast pressure control. Compare the performance of your controller with current practice (PI-control) in simulations.
4. Test your controller in the lab – compare with PI-control.
5. Write a report.

Supervisor: Professor Ole Morten Aamo

ABSTRACT

In drilling operations, it is of great importance to efficiently and safely control the pressure in the well. To avoid possible damage to the reservoir, equipment, personnel and the environment, the pressure in the well bore must be kept within certain limits, determined by the formations around the well. An emerging drilling technique, intended to increase the efficiency and safety of drilling operations, is known as Managed Pressure Drilling (MPD). MPD differs from conventional drilling by closing the mud system with a controlled choke, often in combination with a backpressure pump to ensure circulation through the choke. The controller objective is to automatically adjust the choke to reach the desired downhole pressure. For optimal control of the downhole pressure, a model describing the flows and pressures in the well is necessary. A modal discretization method is considered and implemented in this thesis, resulting in a rational approximation of a two-dimensional distributed parameter model. The discretized model is used to design a LQG controller, for comparison with a PI controller. Both controllers are implemented in MATLAB to perform computer simulations and experiments in lab. Simulations indicated that the transient response of the LQG stabilized at the desired set-point, more efficiently relative to PI controller. This difference was significantly improved when increasing the length of the simulated well. In experiments performed on a tailor made experimental lab located at NTNU, the performance of the two controllers were about equally great. It is discussed whether the lab is inadequate to demonstrate possible improvements due to the introduction of the two-dimensional model.

SAMMENDRAG

Under boring i olje- og gassindustrien er det svært viktig med sikker styring av trykket i brønnen for å minimere sjansene for skade på reservoar, utstyr, arbeidere og miljø. Trykket i brønnen må være innenfor øvre og nedre begrensninger, bestemt av sedimentene rundt brønnen. En voksende boremetode kalt trykkstyrt boring (MPD) er utviklet for å løse trykkrelaterte problemer. MPD skiller seg fra konvensjonell boring ved å styre borevæsken gjennom en automatisert ventil. Hensikten er å styre ventilåpningen slik at et ønsket trykk i brønnen oppnås. For å oppnå optimal styring av ventilen er det nødvendig med en modell som beskriver flyt og trykk i brønnen. I denne avhandlingen er en modal diskretiseringsmetode benyttet for å utvikle en rasjonell tilnærming til en todimensjonal transmisjonslinjemodell. Den diskretiserte modellen er videre benyttet til å utvikle en modellbasert LQG-regulator, for sammenligning med en konvensjonell PI-regulator. Begge regulatorene er implementert i MATLAB for å utføre simuleringer og eksperimenter i lab. Simuleringene indikerte at LQG-regulatoren stabiliserte nedhullstrykket ved ønsket verdi, mer effektivt enn PI-regulatoren. Denne tendensen ble forsterket ved økt lengden på brønnen. Eksperimenter utført på et laboppsett ved NTNU indikerte at de to regulatorene gav tilnærmet lik trykkstyring. Det er i avhandlingen diskutert om laboppsettet ikke er tilstrekkelig for å påvise eventuelle forbedringer ved å ta i bruk en modellbasert regulator, basert på en todimensjonal modell.

PREFACE

This report is the result of a master's thesis, performed and written during the spring semester 2014. This project completes my MSc in Engineering Cybernetics at the Norwegian University of Science and Technology (NTNU).

I would like to thank my supervisor, Professor Ole Morten Aamo, for suggesting this project, for his commitment to my work and guidance throughout the semester. I also thank PhD Candidate Ulf Jakob F. Aarsnes for sharing valuable knowledge, and PhD Candidate Hessam Mahdianfar for helping out with the IPT-Heave Lab.

Johan Fredrik Holm Totland
Trondheim, June 2014

CONTENTS

1 INTRODUCTION 1
1.1 Motivation . . . 1
1.2 Previous Work . . . 1
1.3 Outline . . . 2
1.4 Task Description . . . 2
2 BACKGROUND ON DRILLING 3
2.1 Drilling Terms and Equipment . . . 3
2.2 Introduction to Conventional Drilling . . . 4
2.3 Managed Pressure Drilling (MPD) . . . 5
2.3.1 Techniques . . . 5
2.3.2 Advantages of MPD . . . 6
2.3.3 Offshore Experiences . . . 7
2.3.4 Control Methods . . . 7
3 EXPERIMENTAL LAB 9
3.1 Connections and Heave . . . 9
3.2 Experimental Setup . . . 9
3.2.1 Components . . . 10
3.2.2 Interface . . . 11
4 MATHEMATICAL MODELING 13
4.1 Hydraulic Transmission Lines . . . 13
4.2 Distributed Parameter Models . . . 14
4.2.1 Two-Dimensional Viscous Compressible Model 15
4.2.2 Analytical Solution . . . 15
4.3 Spectral Methods . . . 16
4.4 The Modal Method . . . 16
4.4.1 Boundary Conditions . . . 17
4.4.2 Ritz Method . . . 17
4.4.3 Rational Approximations and Corrections . . . 18
4.4.4 Model Summary . . . 19
4.5 Frequency Analysis . . . 19
5 CONTROLLER DESIGN 21
5.1 Selecting Model Based Controller . . . 21
5.2 Model Based BHP Controller . . . 21

5.2.1 Controller Objective 22
5.2.2 Controller Implementation 23
5.3 Simple BHP Controller 23
5.4 Choke Controllers 24
5.4.1 Operating the Lab Choke 24
5.4.2 Choke Characteristics 24
5.4.3 Forward Linearization 25
5.4.4 PI Choke Controller 26
5.4.5 Tests in Lab 26
6 SIMULATIONS AND EXPERIMENTS 29
6.1 Basis for Simulations and Experiments 29
6.2 Computer Simulations 30
6.2.1 Controlling BHP in Well Simulations 30
6.2.2 Introducing Model Error 31
6.3 Experimental results 33
6.3.1 Model Based BHP Controller 33
6.3.2 Simple BHP Controller 36
6.3.3 Comparing BHP Controllers 37
7 DISCUSSION 39
8 CONCLUSION 41
BIBLIOGRAPHY 43

LIST OF FIGURES

Figure 1 Schematic of a MPD system 8
Figure 2 Schematic of the experimental setup 11
Figure 3 Interface in SIMULINK 12
Figure 4 Frequency analysis of the modal method . . . 20
Figure 5 Choke characteristics 25
Figure 6 Step input forward linearization 27
Figure 7 Step input PI choke controller 27
Figure 8 Computer simulation SIMULINK diagram . . 30
Figure 9 Simulation of BHP for long and shallow wells 31
Figure 10 Bulk modulus (β) test 32
Figure 11 Kinematic viscosity (ν) test 32
Figure 12 Controller implementation in lab interface . . 34
Figure 13 Experiment with different weights on R 35
Figure 14 Experiment using the forward linearization . . 35
Figure 15 Retuning the PI choke controller 36
Figure 16 Hydrostatic pressure compensation 37
Figure 17 Experiments with different tuning K_i 37
Figure 18 Comparing BHP controllers 38
Figure 19 Comparing choke performance 38

LIST OF TABLES

Table 1 Well bore and drilling fluid parameters 29

LIST OF ABBREVIATIONS

A	Cross sectional area $[m^2]$
β	Effective bulk modulus $[Pa]$
BHA	Bottomhole Assembly
BHP	Bottomhole Pressure
c	Speed of sound $[m/s]$
Γ	Propagation operator
L	Length of transmission line $[m]$
LQG	Linear-Quadratic-Gaussian (Controller)
MPC	Model Predictive Control
MPD	Managed Pressure Drilling
NPT	Non-Productive Time
ν	Kinematic viscosity $[Pa \cdot s]$
P, p	Pressure $[Pa]$
PI	Proportional-Integral (Controller)
Q, q	Volumetric flow $[m^3/s]$
ρ_0	Mean fluid density $[kg/m^3]$
s	Laplace operator
T	Propagation time $[s]$
Z_0	Line impedance
Z_c	Characteristic impedance
Z_L	Load impedance

1 INTRODUCTION

1.1 MOTIVATION

In drilling operations performed in the oil and gas industry it is important to control the pressure in the well for safe and efficient drilling. During the operation a drilling fluid, called mud, is pumped into the well serving various purposes, including pressure control. Today, most 'easily drilled' wells have already been drilled and the oil and gas industry is faced with complex drilling operations where the pressure limits are narrow. Difficult pressure margins require safe, efficient and precise pressure control. A series of techniques designed for this purpose is known as Managed Pressure Drilling (MPD). The principle of a MPD technique called Constant Bottom Hole Pressure (CHBP) is to control the pressure in the well by closing the mud circulation with a controlled choke. The control objective is to automatically adjust the choke to reach a desired bottomhole pressure set-point. A model describing the pressure and flow in the mud is necessary to achieve optimal pressure control. Simple lumped parameter models are often applied for this purpose [14, 15, 16], but it is anticipated that an improved model could enhance the performance. The model must captures the dominating dynamics in the well and at the same time be simple enough for control applications.

1.2 PREVIOUS WORK

During the fall semester a project work was conducted by the author regarding review, implementation and simulation of a discretized well model, developed using a Galerkin method [25]. Simulations and frequency analysis was performed to compare the method with a simple control volume method. The Galerkin method is applied in this thesis and parts of the derivations from the project are therefore revised in this thesis.

1.3 OUTLINE

The reader is in Chapter 2 introduced to conventional drilling and the emerging drilling technology managed pressure drilling, which forms the basis for the experimental setup of the presented in Chapter 3. Background for modeling and analytically solving hydraulic systems is presented in Chapter 4 in addition to a numerical approximation known as the modal method. This method is further used to obtain a model fit for controller design, developed in Chapter 5. In Chapter 6 the controller designs are tested and compared in computer simulations and experiments conducted at the lab. The results are discussed in Chapter 7 before the thesis is concluded in Chapter 8.

1.4 TASK DESCRIPTION

1. Review current practices for pressure control in MPD.
2. Review modeling from the project work. Revise the model, if necessary.
3. Suggest a model based control design procedure for fast pressure control. Compare the performance of your controller with current practice (PI-control) in simulations.
4. Test your controller in the lab – compare with PI-control.
5. Write a report.

2

BACKGROUND ON DRILLING

The purpose of this chapter is to serve as a brief introduction to conventional drilling in marine environments and to the drilling method Managed Pressure Drilling (MPD). The content of this chapter is mainly based on Devereux [7] and Rehm et al. [21].

2.1 DRILLING TERMS AND EQUIPMENT

This section provides a short explanation of different terminologies and equipment necessary for understanding drilling operations. For the remaining parts of this thesis, these terms will be commonly used and assumed familiar with the reader.

RIG: a complete installation with equipment needed for a drilling operation. Marine rigs are classified as floating rigs such as semisubmersibles and drill ships, or as bottom supported rigs such as jackups and platforms.

DRILLPIPE: a string consisting of several connected joints. The joints are hollow, thick-walled steel pipes most commonly about 9.5 meters long.

DRILL BIT: a device placed in the lower end of the drillpipe, designed for cutting different rock formations. Drill bits are divided in two types – fixed cutter bits and roller cone bits.

BOTTOMHOLE ASSEMBLY (BHA): a tool extending from the drill pipe to the drill bit. The BHA can be configured in many ways to improve the drilling operation.

DRILLSTRING: the drillpipe, drill bit and BHA connected is referred to as drillstring.

CASING: a steel pipe lowered into the well and cemented in place. The purpose of a casing is to withstand difficult pressure limits.

The drilling continues with a smaller drill bit from the casing point (the lower end of the casing).

DRILLING MUD: a fluid (often water, oil or a combination) pumped through the drillstring into the bottom of the well serving several purposes, e.g. pressure control, stabilize wellbore, remove cuttings, minimize damage to reservoir and cool down drill bit. The properties of the mud must be correct for safe and efficient drilling.

ANNULUS: the space between the drillstring and the inside of the well where the mud carry cuttings away from the hole.

2.2 INTRODUCTION TO CONVENTIONAL DRILLING

In order to produce oil and gas from offshore reservoirs, conventional drilling technologies have developed over the years. A drilling operation is managed and operated from a drilling rig. Drives, pumps and other equipment needed for the drilling operation is installed on the rig and controlled by field engineers and operators. The drillstring with the drill bit rotates and penetrates the seabed by cutting rock formations, creating the well. While drilling, mud is pumped into the drillstring to the bottom of the well and returned through the annulus. One of the main challenges related to drilling is to maintain the pressure in the well within certain boundaries. These boundaries (known as the pressure window) are determined by the fracture pressure, the pressure inside the well that would fracture the surroundings, and the pore pressure, the pressure in the fluids within the pore spaces. If the pressure in the well increase above the fracture pressure, drilling mud will leak into the reservoir formations, causing fractions in the rock surrounding the well. If the pressure decrease below the pore pressure, unwanted fluids and sediments will enter the well from the surroundings. Without sufficient control of the pressure in the well, a blowout could potentially occur, releasing uncontrolled oil and gas to the surface. The results of a blowout could be disastrous. In 2010, the Macondo blowout in the Gulf of Mexico resulted in loss of 11 lives and an enormous oil spill of nearly 5 million barrels [18]. A conventional technique for controlling the bottomhole pressure (BHP) is to add chemicals and weighting mate-

rials to change the hydrostatic pressure in the well. This is a slow and time consuming method which increases non-productive time (NPT). Another technique involves adjusting the mud circulation rate to control the frictional pressure, leading to an increased or decreased bottomhole pressure. A disadvantage of this method is lack of pressure control in case of no circulation.

2.3 MANAGED PRESSURE DRILLING (MPD)

Drilling operations are normally very costly and the oil and gas industry is therefore searching for new technologies to improve drilling and minimize economical costs. With conventional drilling, situations such as differentially stuck pipe, circulation loss, pressure control issues and narrow pressure margins significantly delay drilling operations, resulting in large economic losses. Today, the average non-productive time for wells in Europe is 20-25% [12] and reports from gas wells drilled in the Gulf of Mexico between 1993 and 2003 indicated that 40% of all NPT was related to drilling operations and procedure [21]. The drilling discipline Managed Pressure Drilling (MPD) is a result of the high costs related to NPT. The International Association of Drilling Contractors (IADC) has defined MPD as *an adaptive drilling process used to more precisely control the annular pressure profile throughout the wellbore. The objectives are to ascertain the downhole pressure environment limits and to manage the annular hydraulic pressure profile accordingly* [21].

2.3.1 *Techniques*

Managed pressure drilling is a discipline covering different methods for well pressure management. The most common are

DUAL GRADIENT DRILLING (DGD): a drilling operation where the mud is returned to the rig through one or more small-diameter lines, or dumped at the sea floor. The mud is removed from the well annulus through a mud-lift pump, and by adjusting the pump inlet pressure, the hydrostatic pressure in the well can be controlled.

PRESSURIZED MUD-CAP DRILLING (PMCD): a technique which implies severe losses of mud. When mud is lost to the formation, seawater with additives is applied as drilling mud to force mud and cuttings into the zones where the losses occurred. The BHP is maintained by applying a back pressure.

CONSTANT BOTTOM-HOLE PRESSURE (CBHP): involves controlling the mud with a choke, resulting in a closed mud system. The effective BHP is then given by a sum of the hydrostatic pressure, the choke pressure and the frictional pressure (known as ECD). A backpressure pump is often applied to provide a pressure drop over the choke, resulting in a controllable pressure device for compensation of lost frictional pressure in case of no circulation.

RETURNS FLOW CONTROL (HSE): implies closing the mud returns on the rig floor with a purpose to enhance health, safety and environmental issues.

2.3.2 *Advantages of MPD*

In 2005, at least 50% of all offshore drilling prospects were considered economically not drillable with conventional drilling methods [13]. The advantage of MPD versus conventional drilling is to reduce drilling costs due to NPT while increasing the safety of the drilling operation [21]. With conventional methods, casing is the solution when exposed to difficult pressure margins. However, casing is a time consuming process, and for each casing point, the hole size is reduced. The increased pressure controllability introduced by MPD can allow for extended casings with and a lower number of casing points. Another advantage of a more precise pressure management is avoiding circulation loss, a major cause of NPT. Such losses occur when mud weight is increased to the point when the pressure in the well exceed the fracture pressure. Differential sticking is *a condition whereby the drillstring can not be moved along the axis of the wellbore. Differential sticking typically occurs when high-contact forces caused by low reservoir pressures, high wellbore pressures, or both, are exerted over a sufficiently large*

area of the drillstring[1]. In case of differentially stuck pipe, drilling operations often encounter significant delays, thus non-productive time increases. With MPD, the differential pressure can be controlled to prevent sticking pipe. In addition to the exampled mentioned, drilling with a closed mud system has several advantages related to drilling fluid economics and increased safety for personnel and equipment.

2.3.3 *Offshore Experiences*

The number of wells drilled using MPD has increased rapidly over the last years. Only in Asia Pacific, more than 100 wells were successfully drilled using MPD between 2005 and 2009 [20]. These experiences demonstrated that a closed mud circulation system has numerous advantages and that MPD delivered significant cost savings by eliminating non-productive time associated with fluid losses and well control. In the Kvitebjørn field in the northern North Sea, MPD allowed safe drilling of wells that otherwise not could have been drilled [12]. Another successful MPD operation was the first pressurized mud-cap drilling from a floating rig, conducted offshore Malaysia in 2004 [13]. The operation avoided loss of costly drilling fluid and significantly reduced NPT.

2.3.4 *Control Methods*

From an operator's perspective, MPD introduces additional complexity to a drilling operation, requiring extended coordination of pumps, chokes, valves and more. For an automation engineer, on the other hand, this motivates the need for automatic control. Research related to MPD is often subject to developing control methods. More than 90% of all industrial control loops are based on simple linear PID controllers [12], and the oil and gas industry is no exception. The advantage of PID controllers is the simplicity related to both implementation and tuning, in addition to provide a sufficient solution for most industrial control problems. The complexity of MPD requires different layers of control to ensure an optimal process. A multi-level control hierarchy is presented in [5], typically with PID controllers on

1 Schlumberger Oilfield Glossary

a feedback control level, to execute given set-points, and a model predictive controller (MPC), determining optimal controller set-points based on constraints given by human input. The use of MPC as an optimal model based controller is common for MPD related research [3, 5, 12, 19].

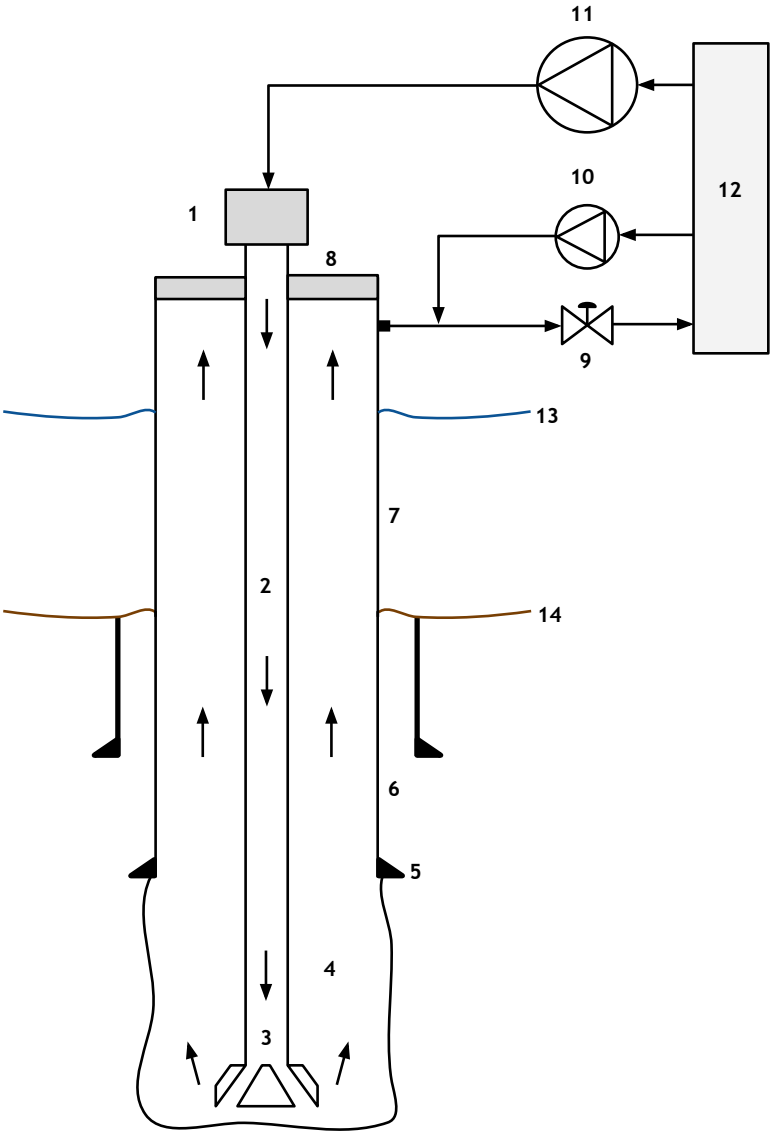

Figure 1: Schematic of a MPD system. [1] Top drive [2] Drillstring [3] Drill bit [4] Annulus [5] Casing [6] Casing point [7] Marine raiser [8] Rotating Control Device (RCD) [9] Choke [10] Backpressure pump [11] Mud pump [12] Mud tank [13] Sea level [14] Sea bed

3

EXPERIMENTAL LAB

A tailor made lab known as *IPT-Heave Lab*, located at the Department of Petroleum Engineering and Applied Geophysics at NTNU, is in this thesis used for experimental purposes. The background for and development of the IPT-Heave Lab is extensively covered by various theses [2, 4, 8, 10, 11]. This chapter serves only as a brief explanation of the experimental setup. For further investigation and a user guide to the lab, the reader is referred to Albert [2].

3.1 CONNECTIONS AND HEAVE

When the drill string is to be extended for deeper penetration, new joints are connected on top of the drill pipe. This scenario is known as *connections* and involves ramping down the mud pump, for then to be disconnected from the drillstring. When drilling from floating rigs, heave effects from waves are compensated to ensure a steady position for the drill bit. During connections, on the other hand, the drill string is fastened to the rig, resulting in rig heave movement being transferred to the drillstring. In this case, the drill bit traverse vertically, leading to pressure fluctuations in the well. The MPD technique constant bottomhole pressure (CBHP) is a possible solution to ensure a constant pressure in the well, regardless of the drill bit movement.

3.2 EXPERIMENTAL SETUP

The IPT-Heave Lab is a tailor made well experiment built for simulation of heave during joint connections from a floating rig. The MPD technique CBHP is the basis for the lab, with a controller objective to control a choke for suppression of wave disturbance and maintaining a given bottomhole pressure (BHP) set-point. The IPT-Heave Lab is a scaled model, originally based on a vertical 4000 meters deep well

with a well bore diameter of 8.5 inches, exposed to heave of amplitude 1.5 meters. A schematic of the experimental setup is shown in Figure 2 and the different components are described in the following section.

3.2.1 *Components*

COPPER PIPE To simulate the flows and pressures in the drilling mud from the bottom of the well to the rig, 900 meters of copper pipe is coiled to form a 2.3 meter high cylinder.

PISTON The bottom of the well is modeled with a vertical PVC pipe, connected to the end of the copper pipe. In order to see the BHA inside the well, the pipe is made with a transparent material. The BHA is vertically moved by an electrical motor driving a saw tooth belt to simulate heave.

CHOKE The choke is tailor made with a electrical motor turning a valve from 0 to 90 degrees, corresponding to closed and fully open respectively.

BACKPRESSURE PUMP A backpressure pump is installed to provide a constant flow, ensuring a necessary pressure drop over the choke. The pump delivers approximately 31 l/min when running on full.

WATER TANK Water is used as drilling fluid in the lab. The supply for the backpressure pump is an open plastic tank, installed with a feeding pump to ensure sufficient supply for the backpressure pump.

SAFETY/MANUAL VALVES To avoid damage to lab equipment and personnel, automatic safety valves are installed to release critical pressures from the system. Manual valves are installed to drain water from the lab if necessary.

FLOW TRANSMITTERS Three flow transmitters are installed at the lab to measure flow at the end of the copper pipe, through the choke and flow rate delivered from the back pressure pump.

PRESSURE TRANSMITTERS Pressure transmitters are installed in the top and at the bottom of the well, at the inlet and outlet of the choke and for every hundred meters of copper pipe.

3.2.2 *Interface*

The lab interface is implemented with the SIMULINK toolbox in MATLAB r2012b on a Windows 7 computer. Measurement signals and control output signals are communicated in real-time through a control card from National Instruments with 32 analog inputs and 4 analog outputs. The SIMULINK interface is shown in Figure 3 where the real-time communication for reading measurement and applying control signals is implemented in the *System*-block. The *Controller*-block is used for choke and piston controller implementation, using measurements as feedback inputs. A safety module is implemented to avoid large pressures and vacuum in the lab. The bottomhole pressure P2 is controlled and experiments are automatically stopped if P2 is above 10.5 bar or below -0.5 bar.

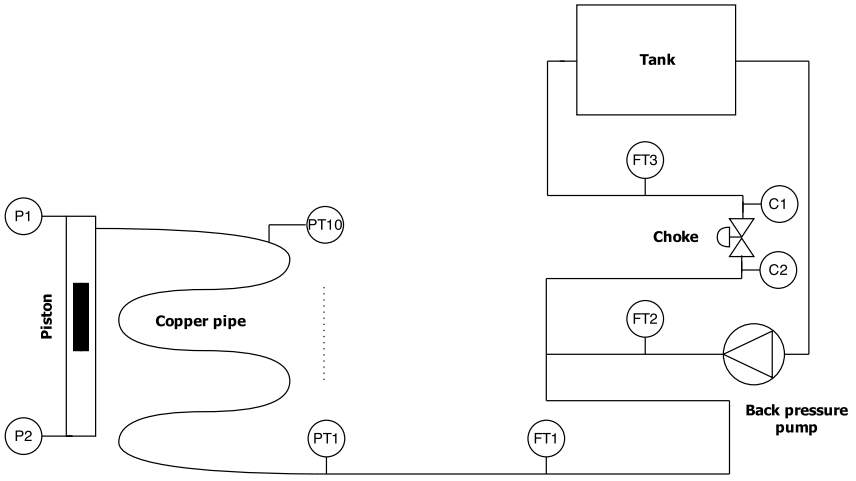

Figure 2: Schematic of the experimental setup

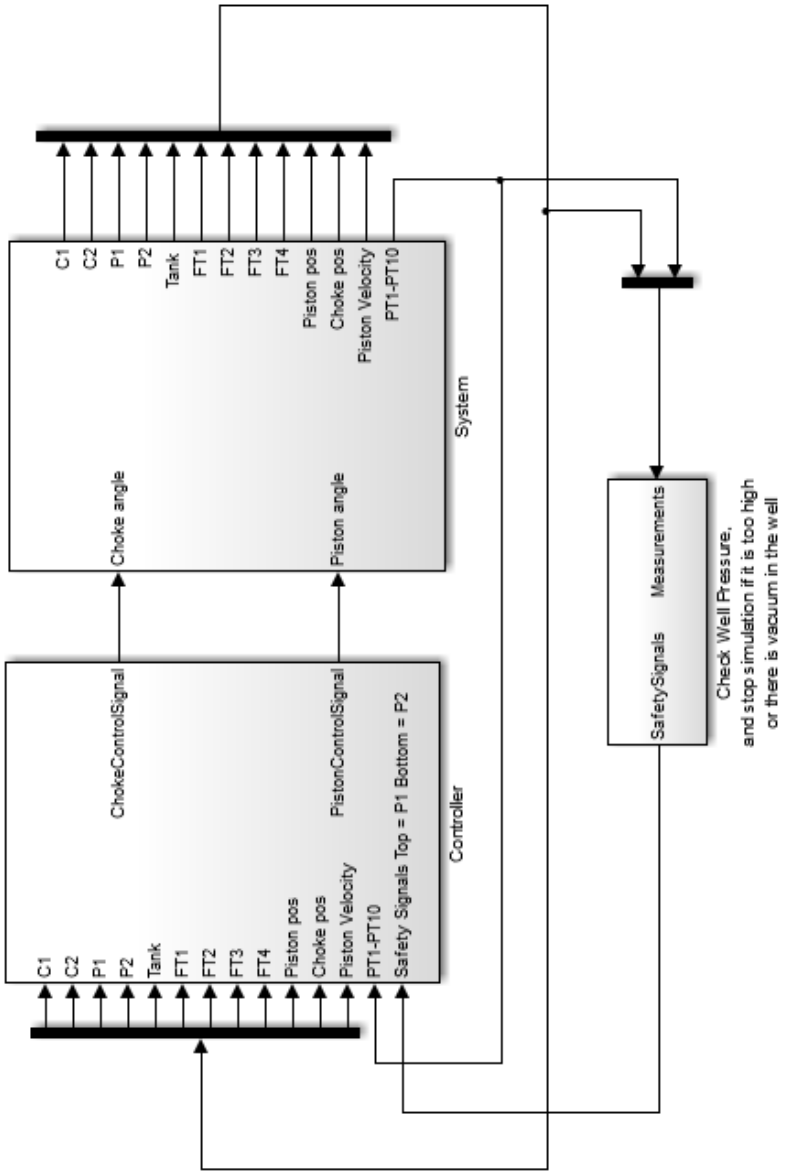

Figure 3: Interface in SIMULINK

4

MATHEMATICAL MODELING

The use of mud during a drilling operation can mathematically be treated as a hydraulic system. By modeling the mud in the well as a hydraulic transmission line, the pressure and flow in the fluid is considered for the whole space, for all time. This is desired when modeling viscous and compressible fluids in long pipes, e.g. mud in a drillstring. This chapter serves as an introduction to hydraulic transmission lines, before a mathematical modal method for obtaining a numerical solution to a transmission line model is presented. The content of the first sections in this chapter is based on Egeland and Gravdahl [9], Stecki and Davis [23] and Canuto et al. [6].

4.1 HYDRAULIC TRANSMISSION LINES

A dynamic model of a hydraulic transmission line is derived in [9]. The model is obtained by considering mass balance and momentum balance on differential control volumes Adx where A is the cross sectional area and $x \in \{0, L\}$ is the spatial coordinate. By considering an infinite number of control volumes the dynamics in the transmission line turn out to be given by the partial differential equations (PDEs) in (1) where $p(x,t)$ is the pressure in the fluid and $q(x,t)$ is the volumetric flow. The properties of the fluid are determined by the bulk modulus β and the density ρ_0, which is assumed to be constant.

$$\frac{\partial p(x,t)}{\partial t} = -cZ_0 \frac{\partial q(x,t)}{\partial x} \tag{1a}$$

$$\frac{\partial q(x,t)}{\partial t} = -\frac{c}{Z_0} \frac{\partial p(x,t)}{\partial x} - \frac{F[q(x,t)]}{\rho_0} \tag{1b}$$

The friction term F is assumed to be a function of $q(x,t)$. Z_0 is the known as the line impedance and c is the speed of sound.

$$Z_0 = \frac{\rho_0 c}{A}, \quad c = \sqrt{\frac{\beta}{\rho_0}}$$

The PDEs (1) are Laplace transformed into equation (2) and a propagation operator Γ is defined by (3).

$$sP(x,s) = -cZ_0 \frac{\partial Q(x,s)}{\partial x} \tag{2a}$$

$$sQ(x,s) = -\frac{c}{Z_0}\frac{\partial P(x,s)}{\partial x} - \frac{F[Q(x,s)]}{\rho_0} \tag{2b}$$

$$\frac{Z_0\Gamma^2(s)}{LTs}Q(x,s) = \frac{Z_0 s}{c}Q(x,s) + \frac{Z_0 F[Q(x,s)]}{c\rho_0} \tag{3}$$

By defining the propagation operator, the transformed model can be written in the form of wave equations (4) where L is the length of the line and $T = L/c$ is the propagation time.

$$\frac{\partial Q(x,s)}{\partial x} = -\frac{Ts}{LZ_0}P(x,s) \tag{4a}$$

$$\frac{\partial P(x,s)}{\partial x} = -\frac{Z_0\Gamma^2(s)}{LTs}Q(x,s) \tag{4b}$$

The transmission line model (4) is completed by choosing the desired friction model, which determines the propagation operator. Various friction models can be derived by considering the fundamental equations of fluid dynamics with different initial assumptions. This is further investigated in the following sections.

4.2 DISTRIBUTED PARAMETER MODELS

The transmission line model found in Section 4.1 is known as a distributed parameter model since it is represented by PDEs. Stecki and Davis [23, 24] presents seven distributed parameter models and the corresponding analytical solutions. The models are derived from the state equation, the continuity equation, the Navier-Stokes equations and the energy equation, all fundamental equations in fluid dynamics. Various assumptions are made for the seven different models, sorted hierarchically based on how closely they resemble the fundamental equations. This property generally implies that the higher order models are more accurate than the lower. The presented models include, from higher to lower order, *'Exact' first-order model, Two-dimensional thermal viscous compressible model, Two-dimensional viscous compressible model, Two-dimensional viscous incompressible model, One-dimensional viscous compressible model, One-dimensional linear resistance compressible model* and *One-dimensional inviscid compressible model*.

4.2.1 *Two-Dimensional Viscous Compressible Model*

Stecki and Davis [23] concluded that the two-dimensional viscous compressible model is considered to be *the most suitable for modeling alternating flow systems with 'long' transmission lines*. The friction model is based on the fundamental equations given in (5). Compared to a simpler one-dimensional model, the two-dimensional model do to a greater extent account for viscous effects.

$$\frac{\partial q}{\partial t} = -\frac{A}{\rho_0}\frac{\partial p}{\partial x} + \frac{\mu_0}{\rho_0}\left(\frac{\partial^2 q}{\partial r^2} + \frac{1}{r}\frac{\partial q}{\partial r}\right) \tag{5a}$$

$$\frac{\partial \rho}{\partial t} = -\frac{\rho_0}{A}\frac{\partial q}{\partial x} - \rho_0\left(\frac{\partial v}{\partial r} + \frac{v}{r}\right) \tag{5b}$$

4.2.2 *Analytical Solution*

The analytical solutions to the models are given in terms of complex functions, namely the propagation operator Γ and the characteristic impedance Z_c. In transmission lines where both downstream and upstream traveling waves are present, the relation between pressures and flows at the two ends of the line can be expressed by

$$P_1 = P_2 \cosh\Gamma + Q_2 Z_c \sinh\Gamma \tag{6a}$$

$$Q_1 = \frac{P_2}{Z_c}\sinh\Gamma + Q_2 \cosh\Gamma \tag{6b}$$

For the two-dimensional viscous compressible model, the propagation operator is stated in (7a). The characteristic impedance is related to the propagation operator according to (7b).

$$\Gamma(s) = Ts \Big/ \sqrt{1 - \frac{2J_1(\kappa)}{\kappa J_0(\kappa)}} \qquad \kappa = jr\sqrt{s/\nu} \tag{7a}$$

$$Z_c(s) = \frac{Z_0}{Ts}\Gamma(s) \tag{7b}$$

In (7a) J_0 and J_1 are Bessel functions of the first kind with order zero and one, respectively. The propagation operator (7a) is irrational and there is a need for a rational approximation to derive a model for simulation and control purposes. This is further investigated when developing a numerical solution.

4.3 SPECTRAL METHODS

There exists several methods for obtaining numerical solutions to differential equations for simulation and control purposes. Spectral methods is a widely used class of such methods. *Spectral methods may be viewed as an extreme development of the class of discretization schemes for differential equations known generically as the method of weighted residuals* [6]. Key elements for these methods are the trial and test functions. The trial functions defines the basis functions used in the series expansion forming the solution. The test functions are used to ensure that the solution satisfies the differential equations with a minimal error. Unlike finite-element and finite-difference methods, spectral methods apply global infinitely differential trial functions, e.g. trigonometric functions. The choice of trial and test functions distinguish the common spectral schemes Galerkin, collocation and tau method. The Galerkin method is probably the most esthetically pleasing method since the test functions are the same as the trial functions. Mäkinen et al. [17] use a Galerkin approach to derive what is referred to as the modal method, for approximating distributed parameter models. In a comparison study of numerical solution methods for transmission lines by Watton and Tadmori [26], the modal method is concluded to be the most accurate, convenient and numerically stable method. The following sections revise the derivations from [17] to develop a model for simulations and controller design.

4.4 THE MODAL METHOD

The following sections are based on the variational modal method presented in Mäkinen et al. [17], used for obtaining discretized numerical models for transient flow simulation in transmission lines. The modal method and the model derivations in [17] has earlier been investigated by the author, during a project work [25]. The model presented in the project is referred to as the Q-model, since the model inputs are given by flow rates at both ends. The following sections present a QP-model with flow rate at one end and pressure at the opposite end as inputs. The QP-model is preferable to the Q-model for applications related to MPD and the experimental IPT Heave-Lab.

4.4.1 *Boundary Conditions*

By combining the equations (4) derived in Section 4.1, the flow rate can be eliminated to form the wave equation (8) with pressure as dependent variable. The boundary conditions for the QP-model are given by the pressure P_1 and the flow rate Q_2 at location $x = 0$ and $x = L$ in the transmission line. Note that the Laplace operator is normalized with $\bar{s} = Ts$.

$$\Gamma^2 P(x,\bar{s}) - L^2 \frac{\partial^2}{\partial x^2} P(x,\bar{s}) = 0 \tag{8}$$

$$P(0,\bar{s}) = P_1, \qquad P'(L,\bar{s}) = \frac{Z_0 \Gamma^2}{L\bar{s}} Q_2 \tag{9}$$

A variational formulation of the wave equation is shown in (10) where (8) is multiplied by the variation δP and integrated by parts.

$$\int_0^L L^2 P' \delta P' + \Gamma^2 P \delta P dx = L Z_0 \frac{\Gamma^2}{\bar{s}} Q_2 \delta P_2 \tag{10}$$

An approximate solution of the wave equation (8) can be obtained by minimizing the quadratic function $I(P)$ (11). In the following section, the Ritz method is applied for this purpose.

$$I(P) = \frac{1}{2} \int_0^L L^2 (P')^2 + \Gamma^2 P^2 dx - L Z_0 \frac{\Gamma^2}{\bar{s}} Q_2 P_2 \tag{11}$$

4.4.2 *Ritz Method*

The Ritz method assumes the solution $\widetilde{P}$ to be in terms of adjustable parameters r_i (Ritz coefficients) shown in (12). The shape functions $\psi_i(x)$ are trigonometric, forming a linearly independent and complete set of functions which satisfies the boundary conditions.

$$\widetilde{P}(x) = P_1 + \sum_{i=1}^{\infty} r_i \psi_i(x) \tag{12a}$$

$$\psi_i(x) = \sin\left(\frac{(2i-1)\pi x}{2L}\right) \tag{12b}$$

With the Galerkin approach, as noted in Section 4.3, the test functions are the same as the trial functions. This implies that the variation δP must satisfy the shape functions $\psi_i(x)$. By applying $\psi_i(x)$ to the quadratic function (11), the Ritz coefficients can be found to be

$$r_i = -\left(\frac{2}{(2i-1)\pi} P_1 + (-1)^i \frac{Z_0}{\bar{s}} Q_2\right) \frac{2\Gamma^2}{\Gamma^2 + \left(\frac{(2i-1)\pi}{2}\right)^2} \tag{13}$$

Giving the approximate solution for P_2 derived from (12a) with $x = L$

$$\widetilde{P}_2 = P_1 + \sum_{i=1}^{\infty}(-1)^{i+1} r_i \tag{14}$$

4.4.3 *Rational Approximations and Corrections*

The solution found using the Ritz method is infinite dimensional and results in irrational transfer functions when applying the propagation operator Γ for the two-dimensional viscous compressible model, presented in Section 4.2.1. This is due to the Bessel-functions. The model must be truncated to a finite number of modes n and the propagation operator must be approximated to obtain a rational solution. In [17], the suggested rational approximation of the propagation operator is based on Woods approximation (15).

$$\Gamma^2(s) = \frac{\bar{s}}{1 - \frac{1}{\sqrt{1+2\bar{s}/\varepsilon}}} \tag{15}$$

This approximation is used to express the irrational terms in (13) with the rational transfer functions shown in (16a). The modal natural frequency ω_i and the damping coefficient ε_i are dependent on the friction coefficient, assumed to be $\varepsilon = 8T\nu/r^2$.

$$\frac{2\Gamma^2}{\Gamma^2 + \alpha_i^2} \approx \frac{2(\bar{s}^2 + \varepsilon\bar{s})}{\bar{s}^2 + \varepsilon_i\bar{s} + \omega_i^2} \tag{16a}$$

$$\alpha_i = \frac{(2i-1)\pi}{2} \tag{16b}$$

$$\omega_i = \alpha_i - \frac{1}{4}\sqrt{\alpha_i\varepsilon} + \frac{1}{16}\varepsilon \tag{16c}$$

$$\varepsilon_i = \frac{1}{2}\sqrt{\alpha_i\varepsilon} + \frac{7}{16}\varepsilon \tag{16d}$$

When the solution is truncated to a finite number of modes, non-physical oscillations known as Gibbs phenomenon will occur if the model input face discontinuities, e.g. step change. This effect is in [17] filtered with attenuation factors w_i. For the QP-model the attenuation factors are given by the Riemann window functions (17b). The attenuation factors apply to the approximate solution $\widetilde{P}$ resulting in the filtered solution $\overline{P}$ shown in (17a).

$$\overline{P}_2 = P_1 + \sum_{i=1}^{n}(-1)^{i+1} r_i w_i \tag{17a}$$

$$w_i = \frac{\sin(\beta_i)}{\beta_i}, \qquad \beta_i = \frac{(2i-1)\pi}{2n+1} \tag{17b}$$

It is necessary to make a small modification to the Γ approximation in order to obtain the correct steady-state pressure. The adjustment applies to the friction coefficient by replacing ε with $b_1\varepsilon$ in (16a) where

$$b_1 = \left(2\sum_{i=1}^{n} w_i/\omega_i^2\right)^{-1} \tag{18}$$

4.4.4 *Model Summary*

Applying the approximations and corrections above, results in the transmission line model shown in (19). By adapting relevant MPD drilling terms, P_1, P_2 and Q_2 are respectively renamed p_c, p_{dh} and q_{dh}, referring to choke pressure and downhole flow rate as inputs, and downhole pressure as output. This rewriting is useful to highlight the connection between the transmission line model and the MPD model, later used for simulations and experiments.

$$p_{dh} = p_c + \sum_{i=1}^{n}(-1)^{i+1} r_i \tag{19a}$$

$$r_i = -\left(\frac{2}{(2i-1)\pi} p_c + (-1)^i \frac{Z_0}{\bar{s}} q_{dh}\right) \frac{2w_i(\bar{s}^2 + b_1\varepsilon\bar{s})}{\bar{s}^2 + \varepsilon_i\bar{s} + \omega_i^2} \tag{19b}$$

4.5 FREQUENCY ANALYSIS

The QP-model can be compared to the exact analytical solution, given in Section 4.2.2, using frequency analysis. The same approach was discussed and applied in the project work [25]. By defining the relation between flow and pressure at location 2 as the load impedance $Z_L = P_2/Q_2$, the solutions found in (6) can be combined to give the following relation at location 1

$$\frac{P_1}{Q_1} = Z_c \frac{Z_L + Z_c \tanh\Gamma}{Z_c + Z_L \tanh\Gamma} \tag{20}$$

Figure 4 presents a frequency analysis of the transfer function (20) with Γ and Z_c corresponding to the two-dimensional viscous compressible model (7). The load impedance $Z_L = 0$ implies constant pressure at the end of the line. For the QP-model, the corresponding frequency response is found considering the transfer function from q_{dh} to p_{dh}. The QP-model is calculated with 2, 4 and 16 modes and the physical parameters are found in Table 1. The peaks indicates

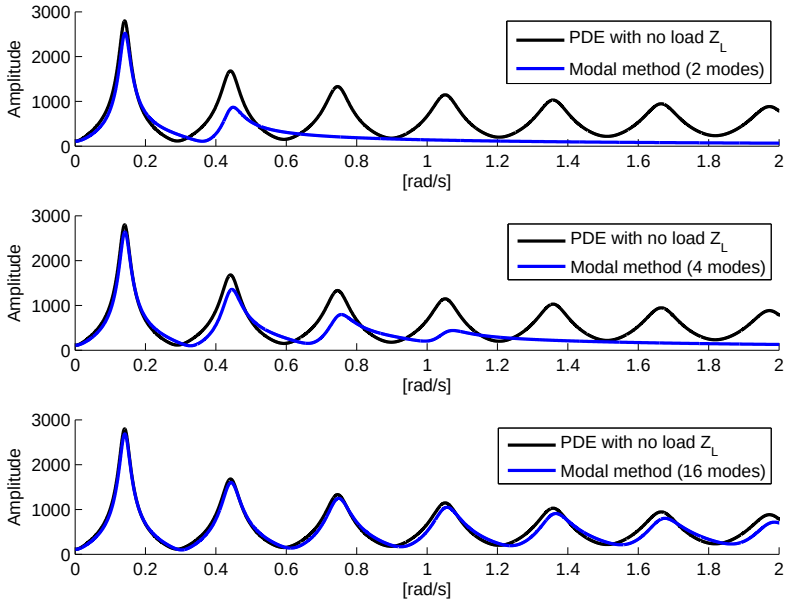

Figure 4: Frequency analysis of the modal method

resonances occurring when the inflow is in phase with the reflected waves. With two modes, the model is relatively accurate at frequencies below 0.3 rad/sec. Adding two more modes increase the accuracy up till 0.6 rad/sec. With 16 modes, the figure indicates that the model is converging toward the exact solution. The frequency analysis indicates similar results as for the Q-model in the project work, where the load impedance $Z_L = \infty$ implied zero flow at the outlet.

5

CONTROLLER DESIGN

One of the main goals of this thesis is to develop a model based bottomhole pressure (BHP) controller, based on the model derived in Section 4.4. In this chapter, both a model based controller and a simple PI controller is developed, for comparison in simulations and lab experiments. Two different choke controllers are developed to handle the nonlinear dynamics introduced by the choke in the experimental lab. Note that u is referred to as system input in Section 5.2-5.3 and as choke opening (in degrees) in Section 5.4.

5.1 SELECTING MODEL BASED CONTROLLER

As noted in Section 2.3.4, model predictive control (MPC) is often preferred for optimal control in MPD. Among several strengths of the MPC is the handling of constraints on inputs and outputs. However, demanding computational calculations is a disadvantage, in addition to a relatively complex implementation. In this thesis, the linear-quadratic-Gaussian regulator (LQG) is selected as control method to design a model based controller. LQG can be considered as MPC without constraints, and implies a simpler implementation where the calculated controller gain is valid for all time. For the purpose of this thesis, LQG is considered to be sufficient for demonstrating the performance of a model based controller, compared with a conventional PI controller.

5.2 MODEL BASED BHP CONTROLLER

Linear-quadratic-Gaussian (LQG) is a result of Wiener's work on optimal filtering from the 1940's, leading to what is known as optimal control [22]. LQG is a composition of the linear-quadratic regulator (LQR) and a Kalman filter for state estimation. LQR is a model based optimal controller, applying the input $u = -K_r x$ where K_r is the con-

troller gain and x is a state feedback from the plant, modeled with the LTI system shown in (21).

$$\dot{x} = Ax + Bu + w \tag{21a}$$

$$y = Cx + Du + v \tag{21b}$$

By solving the algebraic Riccati equation, the optimal state-feedback gain K_r is calculated to minimize the cost function (22) where $Q = Q^T \geq 0$ and $R = R^T > 0$ are weight matrices for the states and input, respectively.

$$J = \int_0^\infty \left(x^T Q x + u^T R u \right) dt \tag{22}$$

The states are often not accessible, and a Kalman filter is therefore applied for state estimation. The optimal state estimate $\hat{x}$ minimize $E\left([x - \hat{x}]^T [x - \hat{x}]\right)$ and is applied to give the optimal controller (23a). The Kalman filter is implemented as shown in (23b).

$$u = -K_r \hat{x} \tag{23a}$$

$$\dot{\hat{x}} = A\hat{x} + Bu + K_f(y - (C\hat{x} + Du)) \tag{23b}$$

A, B, C, D are system matrices for a system on the form of (21) where w and v are assumed to be white noise. The Kalman filter gain K_f is dependent on the noise variance $Q_n = E[ww^T]$ and $R_n = E[vv^T]$.

5.2.1 *Controller Objective*

For the QP-model derived in Section 4.4, the input is $u = \begin{bmatrix} q_{dh} & p_c \end{bmatrix}^T$ and the output is $y = p_{dh}$. The control objective is to control p_c to ensure p_{dh} adjust to the given set-point $p_{dh,ref}$. A possible approach to fulfill this objective is to add a new state $\dot{z} = e = p_{dh,ref} - p_{dh}$, providing the controller with integral action. Adding the integral action results in the following state space representation

$$\begin{bmatrix} \dot{x} \\ \dot{z} \end{bmatrix} = \begin{bmatrix} A & 0 \\ -C & 0 \end{bmatrix} \begin{bmatrix} x \\ z \end{bmatrix} + \begin{bmatrix} B \\ -D \end{bmatrix} u + \begin{bmatrix} 0 \\ 1 \end{bmatrix} p_{dh,ref} \tag{24}$$

The new weight matrix Q is shown in the cost function (24) where only the integrated deviation from the set-point is weighted to ful-

fill the objective of the controller. The new state z is not selected for estimation by the Kalman filter.

$$J = \int_0^\infty \left(\begin{bmatrix} x^T & z^T \end{bmatrix} \begin{bmatrix} 0 & 0 \\ 0 & q \end{bmatrix} \begin{bmatrix} x \\ z \end{bmatrix} + u^T R u \right) dt \tag{25}$$

5.2.2 *Controller Implementation*

The Kalman and LQR gains are calculated with a MATLAB-script using basic predefined functions, and the controller is implemented according to (23) in SIMULINK. The Kalman gain K_f is calculated using the `kalman`-function and the optimal control gain K_r is found using the `lqr`-function. When tuning the LQG controller, Q is selected to be constant with $q = 1$, leaving only the weight R to be adjusted. This approach is valid since the ratio between Q and R is the determining factor affecting the controller gain.

5.3 SIMPLE BHP CONTROLLER

PI (and PID) controllers are by far the most common regulators in industrial control loops. The controller computes an output based on the error e, the proportional gain K_p and integral gain K_i. The integral term reduces the steady-state error by accounting for error accumulated over time. The PI controller is shown in (26). K_p and K_i are tuning parameters necessary to optimize the performance and ensure a stable controller. Several methods are developed for tuning PI controllers. For the purpose of this thesis, it is considered to be sufficient to determine the tuning parameters by trial and error. The controller objective is the same as for the LQG controller – to control the pressure p_{dh} to the given set-point $p_{dh,ref}$ by adjusting p_c.

$$p_c = K_p e + K_i \int_0^t e dt \tag{26a}$$

$$e = p_{dh,ref} - p_{dh} \tag{26b}$$

5.4 CHOKE CONTROLLERS

5.4.1 *Operating the Lab Choke*

The operational area for the tailor made choke at the IPT-Heave Lab is from 0 to 90 degrees, corresponding to closed and fully open. The choke opening is controlled via the lab interface, where the desired opening is converted to the corresponding voltage signal, applied to the motor controller. In this thesis, a cascade approach is considered for controlling the choke. This implies that a low level controller must be implemented to ensure p_c is following the desired $p_{c,ref}$. Two different approaches to this problem are explored in this thesis. Firstly, a forward linearization describing the relation between the choke opening, pressure and flow rate measured in real-time. Secondly, a PI controller using the error $p_{c,ref} - p_c$ to control the opening.

5.4.2 *Choke Characteristics*

To implement the forward linearization, it is necessary to describe the relation between choke opening, flow rate and pressure drop. This relation is for valves often approximated with the functional shown in (27a) where p_c and p_0 is the pressure at the choke inlet and outlet, respectively, and q_c is the flow through the choke. $G(u)$ is a strictly increasing function know as the choke characteristics with the choke opening u as input.

$$q_c = G(u)\sqrt{\frac{p_c - p_0}{\rho}} \tag{27a}$$

$$G(u) = q_c\sqrt{\frac{\rho}{p_c - p_0}} \tag{27b}$$

To approximate $G(u)$ for the lab choke, it is necessary to measure q_c, p_c and p_0 for various choke openings. In the experiment performed to gather necessary data, the choke opening is slowly ramped over a desired operational area. The choke input is slowly ramped to ensure steady conditions in the fluid without including unwanted dynamics. During the experiment, the backpressure pump is constantly running on full, delivering approximately 31 l/min. The choke is slowly closed from 90 to 40 degrees and then reopened to 90 degrees. The

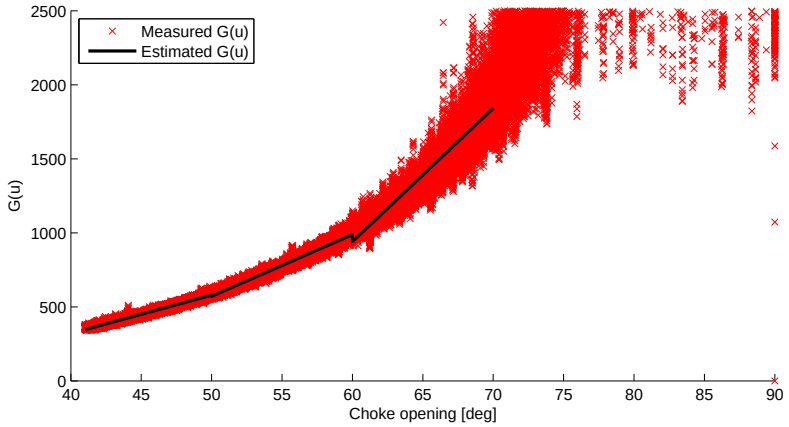

Figure 5: Choke characteristics

opening is not decreased below 40 degrees, to avoid exceeding the safety pressure limits in the lab. $G(u)$ is calculated using (27b) with measured data C1, C2 and FT3 (see Figure 2 for experimental setup). The data is filtered to remove measurement noise. Inspired by [2], the pressures are filtered with $\frac{50}{s+50}$ and the flow rates are filtered with $\frac{20}{s+20}$. Figure 5 shows $G(u)$ calculated with measured data (red).

5.4.3 *Forward Linearization*

The forward linearization is shown in (28). To ease the implementation, the MATLAB function `polyfit` is applied to approximate $G(u)$ with linear functions. Shown in Figure 5, three intervals between 40 and 70 degrees are chosen for approximation of $G(u)$. For most experiments, the lab choke operates between 40 and 60 degrees, corresponding to approximately 7.5 and 1.5 bar downhole. Below 40 degrees, pressure transients and steady-state pressures can potentially increase above the determined pressure limit. Between 70 and 90 degrees, the choke is practically open and the pressure drop over the choke can occasionally be negative due to measurement noise. This effect will cause problems during computations and is therefore avoided with a saturation-block with 70 degrees as upper limit. A linear approximations of $G(u)$ can easily be inverted to obtain the forward linearization (28). By replacing the choke pressure with a pres-

sure reference $p_{c,ref}$, the choke opening can be calculated and applied as a forward controller (28), with q_c and p_0 measured in real-time.

$$u = G^{-1}\left(q_c\sqrt{\frac{\rho}{p_{c,ref} - p_0}}\right) \tag{28}$$

The three approximated linear functions (29) are shown in Figure 5. The controller is implemented with standard blocks in SIMULINK and a tailor made function to automatically swap between the linear approximations, according to the measured choke pressures at $u = 50$ and $u = 60$.

$$G(u) = \begin{cases} 25.9u - 715.9 & u \in [40, 50] \\ 41.7u - 1513.7 & u \in [50, 60] \\ 90.1u - 4465.5 & u \in [60, 70] \end{cases} \tag{29}$$

5.4.4 *PI Choke Controller*

The second alternative developed for controlling choke opening is a simple PI controller, similar to the bottomhole controller developed in Section 5.3. The controller calculates an output choke opening u from the input $e = p_{c,ref} - p_c$. The implementation of the controller is conducted with standard blocks in SIMULINK and the parameters k_i and k_p are tuned by trial and error in lab experiments.

$$u = k_p e + k_i \int_0^t e dt \tag{30}$$

5.4.5 *Tests in Lab*

Both controllers are tested in lab with a step input $p_{c,ref}$, similar to the step test later performed on the downhole pressure controllers. The desired set-point and measured choke pressure for the two alternatives are shown in Figure 6 and Figure 7. The upper figure indicates that the forward linearization do not to reach the desired choke pressure. The PI choke controller is manually tuned during experiments, two of which are shown in the lower figure. The effects of the varying choke performances are shown with closed-loop experiments in the following chapter.

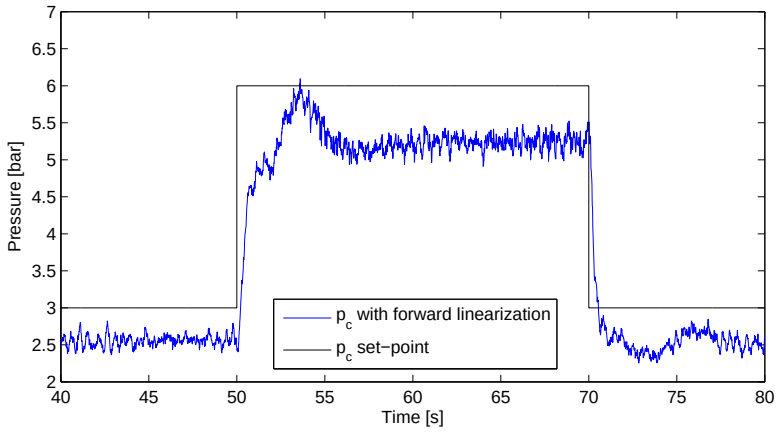

Figure 6: Step input forward linearization

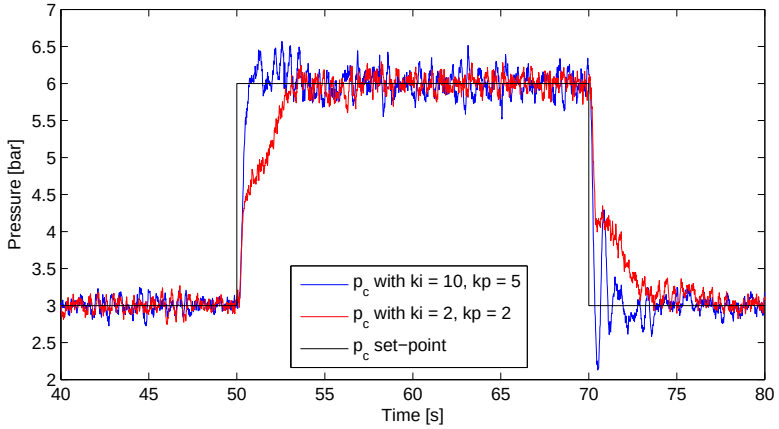

Figure 7: Step input PI choke controller

6

SIMULATIONS AND EXPERIMENTS

This chapter describes and presents both computer simulations and experimental results from the IPT-Heave Lab. The basis for the simulated scenarios is introduced in the following section before simulations results are presented. The main part of this chapter is the presentation of experimental results.

6.1 BASIS FOR SIMULATIONS AND EXPERIMENTS

The main scenario for the simulations is to ramp the downhole pressure reference to increase the pressure set-point. This scenario is relevant when the mud pump is ramped down and disconnected during connections. Using MPD, the pressure formerly imposed by mud circulation and friction can be compensated with the choke pressure to maintain a desired bottomhole pressure (BHP). The experimental setup is designed for simulation of bottomhole heave disturbance during connections and is therefore not configured to apply mud circulation. The simulations are therefore conducted with zero flow rate into the bottom of the well.

	Simulation well	IPT-Heave Lab	
L	10.000	900	$[m]$
r	0.1	0.016	$[m]$
ρ	1420	998.2	$[kg/m^3]$
ν	$30 \cdot 10^{-6}$	$1.004 \cdot 10^{-6}$	$[Pa \cdot s]$
β	$1.4 \cdot 10^{9}$	$2.2 \cdot 10^{9}$	$[Pa]$

Table 1: Well bore and drilling fluid parameters for simulation and lab

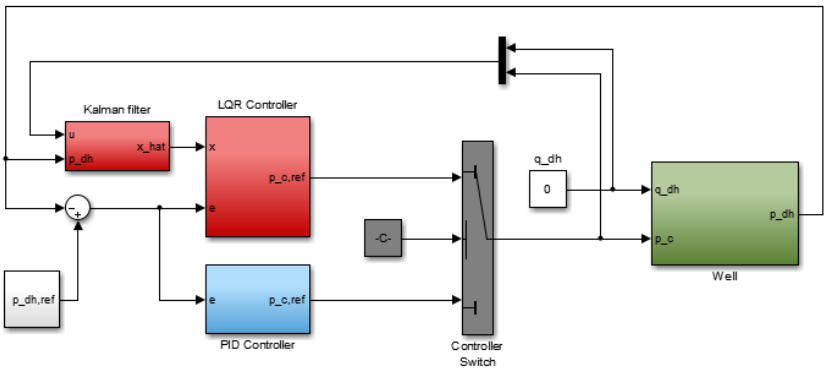

Figure 8: Computer simulation SIMULINK diagram

6.2 COMPUTER SIMULATIONS

The computer simulations are performed with the MATLAB r2013a SIMULINK toolbox on a Windows 7 computer. In the simulations, the process is represented by a high order (24th) QP-model with physical parameters as shown in Table 1. The simulation parameters are inspired by [1]. The QP-model is implemented using the derived transfer functions (19) and converted to a LTI `sys`-object using the `ss`-function. The `sys`-object can easily be implemented in SIMULINK with standard blocks. The model used for controller implementation is a low order (4th) QP-model with the same physical parameters.

6.2.1 *Controlling BHP in Well Simulations*

Figure 9 shows a ramping (2 bar/sec) of the downhole pressure set-point, from 100 to 150 bar. The red line indicates the downhole pressure controlled with LQG, based on a low order model. The blue line indicates the downhole pressure controlled with the PI controller. The upper figure is obtained using a 2.000 meters long well while the lower is 10.000 meters long. For the short well, it takes about 40 sec using LQG and 1 min 40 sec using the PI controller, to reach 150 bar. For the longer well, it takes about 1 min 20 sec using LQG and 5 min using the PI controller. This indicates that the performance of the model based controller is improved for long wells, relatively to the performance of the simple controller. The figure also indicates the increased propagation time for longer wells, considering the downhole pressure transient delay.

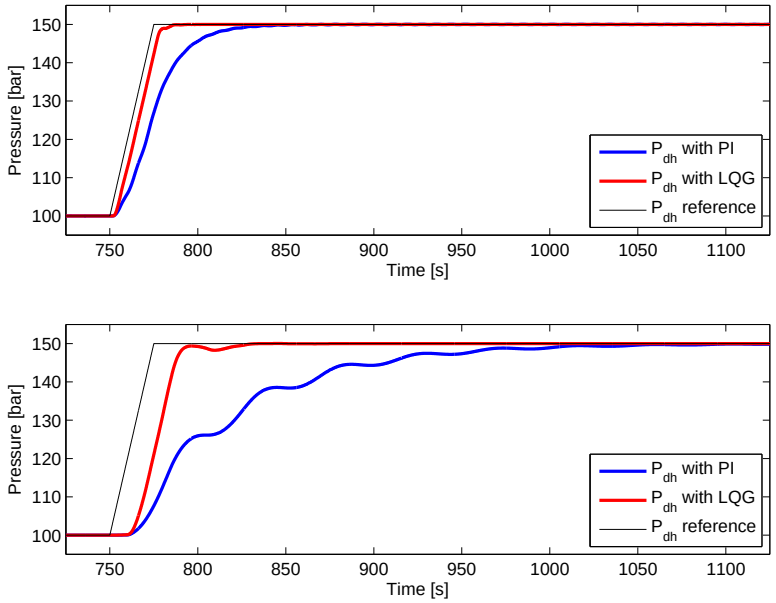

Figure 9: Simulation of P_{dh} for a 2.000 m (upper) and a 10.000 m (lower) well. The pressure is controlled with PI (blue) and LQR (red) controllers

6.2.2 *Introducing Model Error*

A model is not likely to exactly describe the original process. To investigate the performance of the LQG when the model deviates from the process, the mud properties are modified to introduce model error. The bulk modulus β is the most important property in determining the transient response of a hydraulic system [14] and an important aspect is the rapid decrease in the effective bulk modulus when only a small amount of gas is entrained. In Figure 10 the effective bulk modulus is reduced without tuning or adjusting the controller. Introducing a 50% error lead to significant oscillations when ramping the pressure set-point, relative to the case of no or small model error. The kinematic viscosity is another physical parameter which is difficult to determine. In Figure 11, the effective kinematic viscosity is changed with +/- 50% relatively to the model. The error affects the transient response but do not significantly worsen the performance.

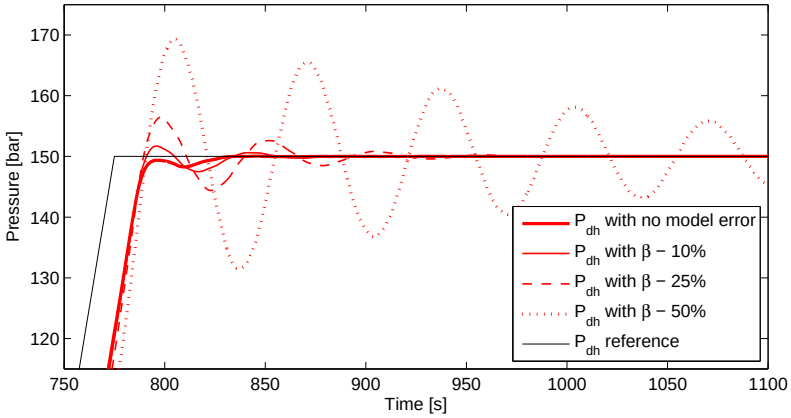

Figure 10: Bulk modulus (β) test where the effective bulk modulus reduced with 10, 25 and 50%

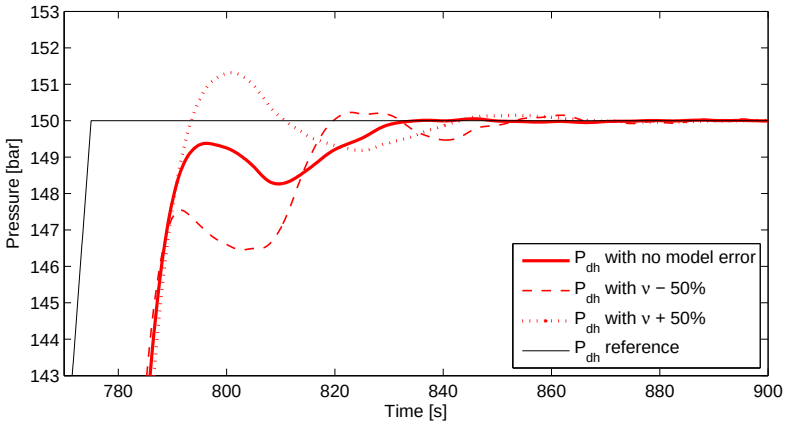

Figure 11: Kinematic viscosity (ν) test where the effective kinematic viscosity is changed +/- 50%

6.3 EXPERIMENTAL RESULTS

The experimental results are obtained using the IPT-Heave Lab introduced in Chapter 3. In the computer simulations, the choke pressure p_c was assumed to perfectly follow the desired controller output reference $p_{c,ref}$, i.e. the nonlinearities normally introduced by a choke was neglected. To perform experiments, the dynamics of the choke must be considered. In Section 5.4, two choke controllers were developed with $p_{c,ref}$ and measurements as inputs, generating the corresponding choke opening u. Both controllers are tested in cascade with the downhole pressure controllers. The controller implementation is seen in Figure 12.

6.3.1 *Model Based BHP Controller*

The following experimental results are obtained using the model based downhole pressure controller, indicated with the red box in Figure 12. The LQG is based on a 8th order QP-model with physical parameters and drilling fluid properties listed in Table 1. The density, viscosity and bulk modulus is based on listed properties for water at 20°C. The length and radius of the copper pipe is found in [2].

6.3.1.1 *Initial Tuning of LQG Weight Parameter*

Figure 13 presents experiments with three different values for the LQG input weight R and a step input on the reference from 3 to 6 bar. The experiments are conducted with the PI choke controller with initial tuning parameters $k_i = 10$ and $k_p = 5$. An increasing weight R implies less use of the output, resulting in a slower response. Using $R = 8$ is considered to give a satisfying performance.

6.3.1.2 *Experiment Using the Forward Linearization*

In Figure 14 the PI controller in the previous experiment is replaced with the forward linearization. Recall from Section 5.4.5 that the forward linearization did not achieve the desired choke pressure $p_{c,ref}$ but in closed-loop, the integral action in the LQG removes most of the steady-state error. However, the transient response is not faster than with the PI controller, and the dependence on measured flow and

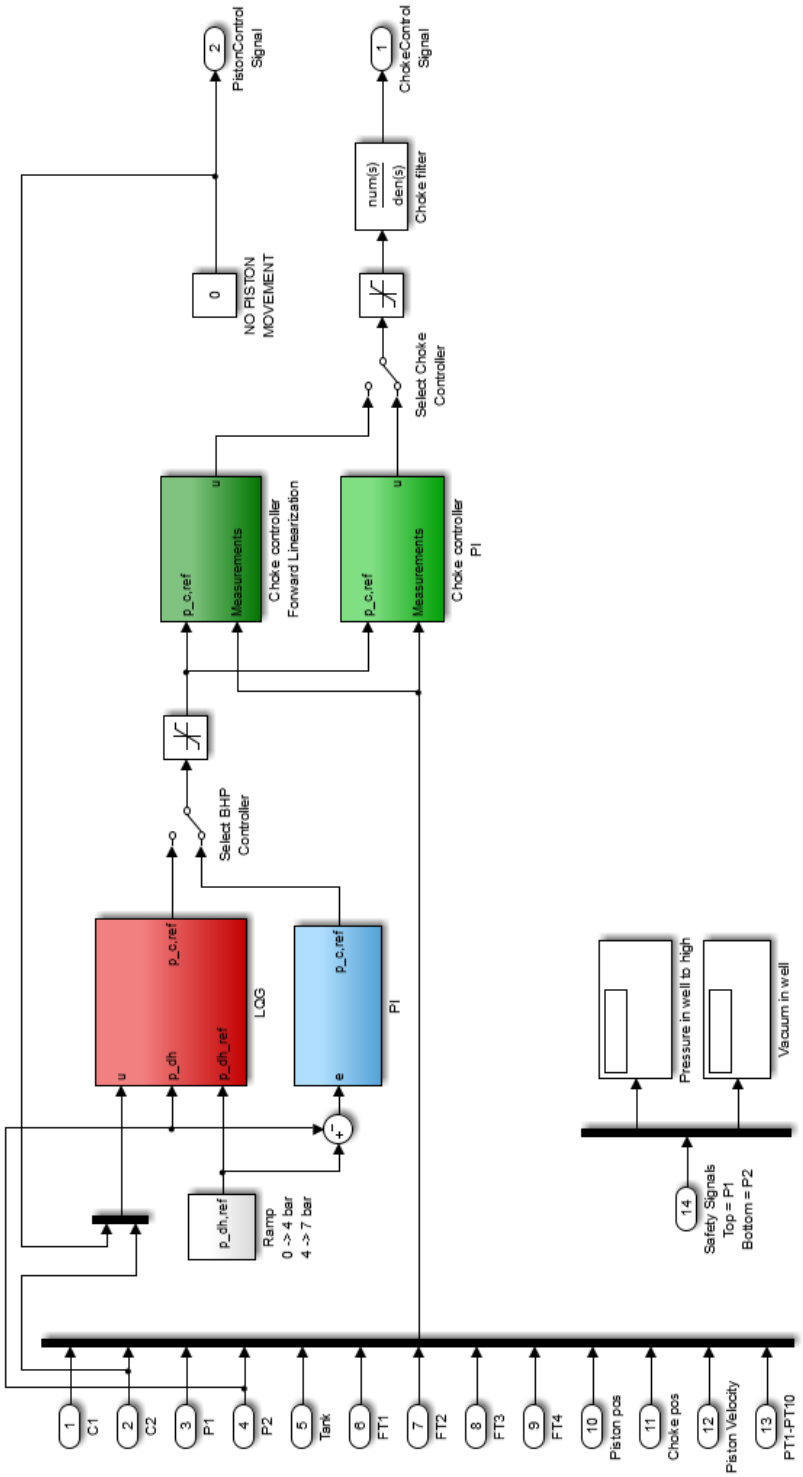

Figure 12: Controller implementation in lab interface

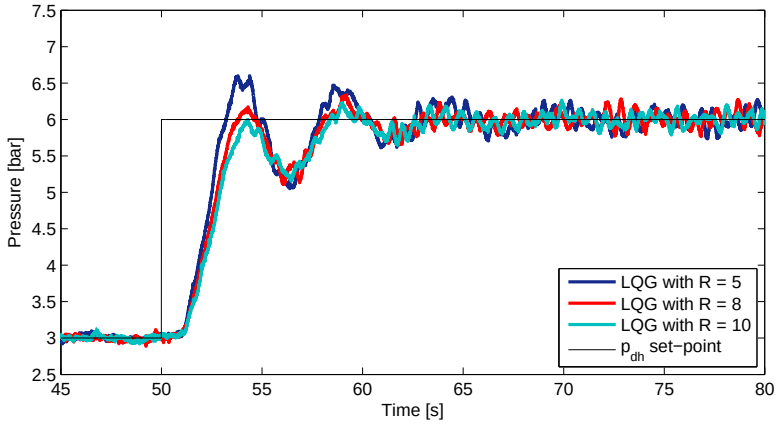

Figure 13: Experiment with different weights on R

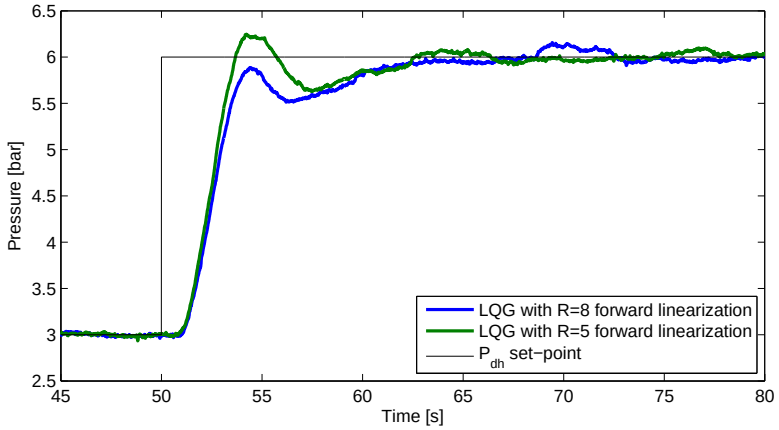

Figure 14: Experiment using the forward lineatization

pressure results in a less robust controller with occasional steady-state errors. The PI controller is preferred in the following experiments.

6.3.1.3 *Retuning the PI Choke Controller*

The results from the LQG tuning motivated for further improvement of the closed-loop performance, by adjusting the choke controller tuning parameters. In Figure 15, the integral gain k_i is adjusted while the proportional gain k_p is held constant. Reducing the integral gain to 2.5 improved the performance of the closed-loop controller. It was further experimented to increase the integral action of the LQG, to compensate for the reduced integral effect of the choke controller. This attempt did not improving the performance. It was also experi-

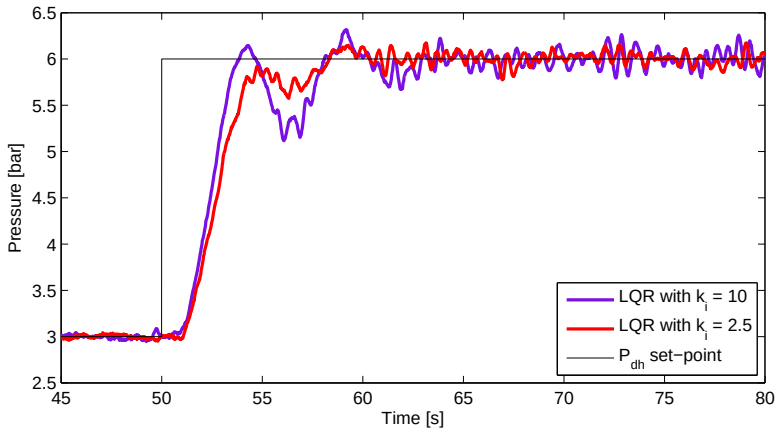

Figure 15: Retuning the PI choke controller

mented to increase the number of modes for the QP-model from 8th to 16th order, without indicating improved performance.

6.3.1.4 *Hydrostatic Feedforward Implementation*

When the experimental lab is in steady-state, a pressure difference between p_{dh} and p_c is measurable. This difference is due to the hydrostatic pressure $p_h = \rho g h$. In the previously conducted experiments, this difference is neglected, implying that the integral action in the controller compensates for the hydrostatic difference. In Figure 16, this difference is implemented as a known disturbance with feedforward, by subtracting p_h from controller input p_{dh} and adding p_h to the controller output $p_{c,ref}$. The figure shows that the known hydrostatic pressure in feedforward did not significantly improve the performance of the transient response. The hydrostatic pressure is calculated with $p_h = p_{dh} - p_c$ when the lab is in steady-state.

6.3.2 *Simple BHP Controller*

The following experiments are conducted with the simple downhole pressure controller developed in Section 5.3, indicated with the blue box in Figure 12.

6.3.2.1 *Tuning PI Controller*

The PI controller was tuned by trial and error with repeating experiments using different values on the integral and proportional gains.

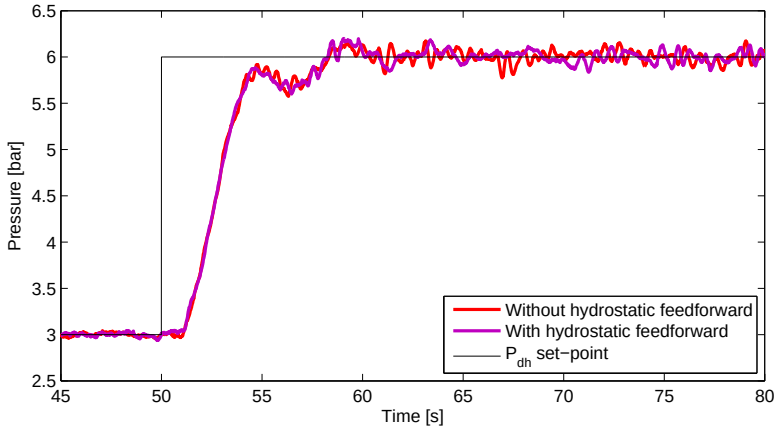

Figure 16: Compensating for hydrostatic pressure difference

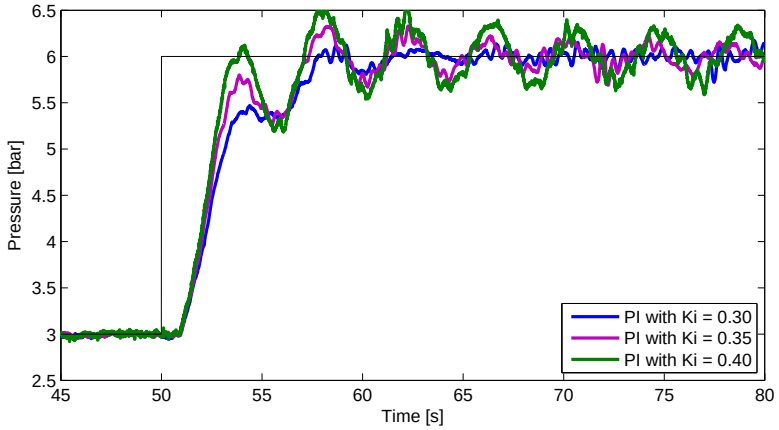

Figure 17: Experiments with different tuning K_i

The experiments shown in Figure 17 are conducted with $K_p = 0.05$ and three different values for K_i. The most satisfying performance is considered to be obtained using $K_i = 0.3$, when emphasizing to reach the desired set-point most effectively.

6.3.3 *Comparing BHP Controllers*

In Figure 18, the most satisfying performances of the two controllers are compared. The figure indicates that both the LQG and the PI controller reach the desired downhole pressure after approximately the same delay. It could be justified to state that the LQG is closer to reaching the desired set-point, when comparing the performances 5 seconds after the step input. However, it is possible that the differ-

ence in performance could decrease with more accurate tuning. The corresponding choke pressure and choke pressure reference from the downhole controllers, is shown in Figure 19. The figure indicates an error for both controllers, possibly affecting the closed-loop performances.

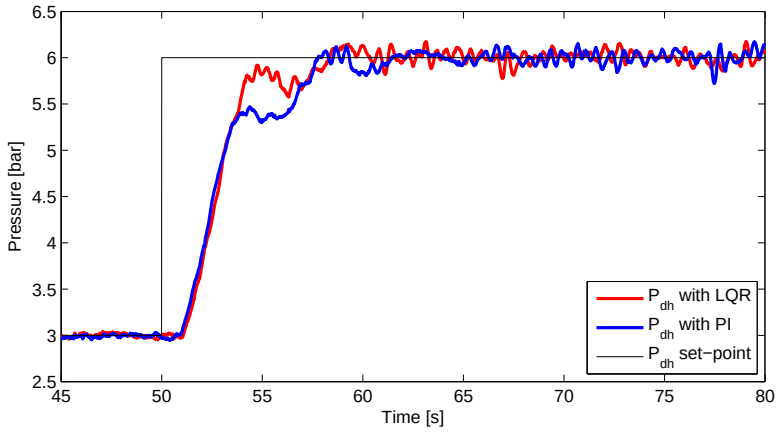

Figure 18: Comparing BHP controllers

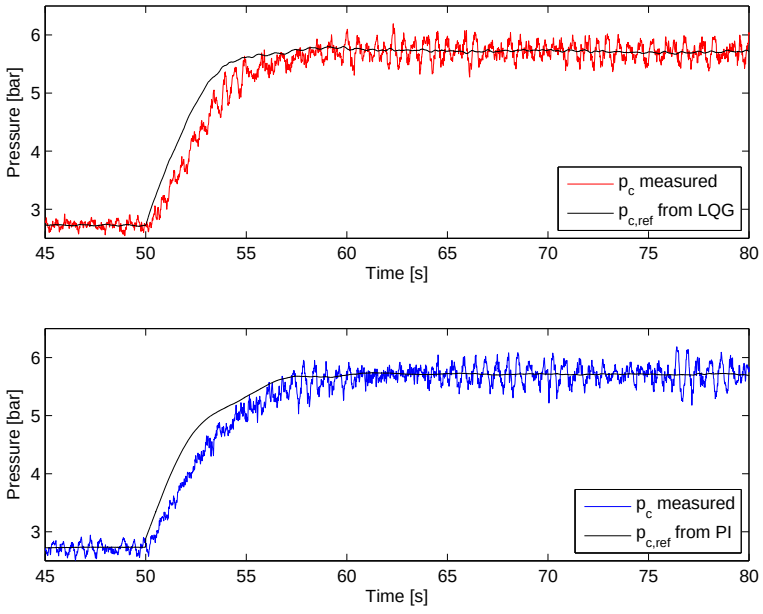

Figure 19: Comparing choke performance for LQG and PI

7

DISCUSSION

The main objective of this thesis was to design a model based controller for controlling the downhole pressure in a well, based on the discretization method presented in Mäkinen et al. [17]. A model based LQG controller was implemented and compared to the well-known PI controller in simulations and in experiments performed in a lab. In simulations, the LQG controller reached the desired downhole set-point ahead of the PI controller. However, experimental results from the IPT-Heave Lab did not show the same significant advantage using the model based controller, relative to the simpler controller.

Different factors could singlehandedly or in combination affect the results found in the performed simulations and experiments. One possible source of error affecting downhole controller lab performance is the behavior of the choke. As shown in Section 5.4.5, the choke was difficult to control for efficiently achieving $p_c = p_{c,ref}$. The PI controller oscillated 0.5 bar from the reference and the forward linearization did not achieve the desired choke pressure. The oscillations could partly be caused by measurement noise. As seen in Figure 7, the pressure oscillations are slightly reduced at lower pressures, with a larger choke opening giving decreased turbulence in the flow at the choke outlet. Integral action in the downhole controller could potentially compensate for the steady-state error caused by the choke, nevertheless, the closed-loop performance indicated that the choke controller did not operate as well as intended. Figure 15 highlights the impacts related to choke tuning and Figure 19 display the difference between the outputs from the BHP controlles and the respective measured choke pressures, indicating a deviation possibly affecting the BHP controller performances.

The IPT-Heave Lab used for experiments in this thesis is only 900 meters long. As shown with simulations, increasing the length of the well from 2.000 to 10.000 meters, significantly improved the LQG performance, relative to the PI controller. This probably implies that the design of the experimental lab makes it difficult to demonstrate the

advantages of introducing a controller based on a discretized two-dimensional viscous compressible model.

In computer simulations, the system used to simulate the well was based on the same QP-model, used to develop the LQG controller. The well was modeled with a 24th order model while the LQG was based on a 4th order system. When applied to a experimental setup, the model will most probably differ from the process. Considering this, the simulation performance of the LQG probably differ further from an expected experimental performance, than the PI controller. However, for small model errors, simulations indicated that the LQG performance remained preferable, relatively to the PI controller.

The basis for the control methods applied during this thesis have been according the current practice, with a low level controller to adjust the choke to the correct pressure, and a higher level controller to determine the choke pressure set-point. To apply this cascade connection, it is critical that the lower level controller is faster than the higher level. Another possible approach to control the downhole pressure in the lab could have been to linearize the choke and merge this with the transmission line model, developing a model based controller with choke opening as output. Whether this method is practically feasible to implement and results in a more satisfying performance, can only be considered as speculations.

8

CONCLUSION

In this master's thesis, a modal method was applied to discrete a two-dimensional viscous compressible model. The discretized model formed the basis for a model based controller, developed for fast pressure control using managed pressure drilling. A model based LQR controller was designed and compared to the well-known PI controller in simulations and experiments.

Simulations indicated that the model based controller stabilized the downhole pressure at the desired set-point, more efficiently than what could be achieved with the PI controller. The LQG performance was further improved when increasing the length of the well, relative to the PI controller. Experiments were performed on a tailor made lab setup known as IPT-Heave Lab. The results from these experiments indicated that the LQG controller was close to reach the set-point before the PI controller but both controllers stabilized at about the same time. In other words, the results did not indicate the same advantage by using the model based controller, as achieved with simulations.

The experimental lab used during this thesis is concluded to be inadequate to demonstrate any significant advantages of introducing a discrete two-dimensional distributed parameters model for controller design. The length of the copper pipe in lab is assumed to be too short, to show any prominent strengths of the model based controller and corresponding weaknesses of the PI controller. As further work, it could therefore be suggested to apply the controller based on the two-dimensional model on a larger scale experimental lab. However, large scale installations are normally very costly, and for the time being, no such facility is available at NTNU.

BIBLIOGRAPHY

[1] Aarsnes, U. J. F., Aamo, O. M., and Pavlov, A. Quantifying Error Introduced by Finite Order Discretization of a Hydraulic Well Model. *Control Conference (AUCC), 15-16 November, Sydney, Australia*.

[2] Albert, A. (2013). Disturbance Attenuation in Managed Pressure Drilling. Master's thesis, Norwegian University of Science and Technology, Trondheim.

[3] Albert, A., Aamo, O. M., Godhavn, J. M., and Pavlov, A. (2014). Disturbance Rejection by Feedback Control in Offshore Drilling: Experimental Results. *The 19th World Congress of the International Federation of Automatic Control, 24-29 August, Cape Town, South Africa*.

[4] Ånestad, J. M. (2013). System Identification and Simulation of an Experimental Setup for Managed Pressure Drilling. Master's thesis, Norwegian University of Science and Technology, Trondheim.

[5] Breyholtz, Ø., Nygaard, G., Siahaan, H., and Nikolaou, M. (2010). Managed Pressure Drilling - A Multi-Level Control Approach. *SPE Intelligent Energy Conference and Exhibition, 23-25 March, Utrecht, The Netherlands*.

[6] Canuto, C., Hussaini, M. Y., Quarteroni, A., and Zang, T. A. (1987). *Spectral Methods in Fluid Dynamics*. Springer-Verlag, Harrisonburg, USA.

[7] Devereux, S. (2012). *Drilling Technology in Nontechnical Language*. PennWell, Oklahoma, USA, 2 edition.

[8] Drønnen, R. T. (2013). Generering av Forstyrrelse i et Eksperimentelt Lab-oppsett for Managed Pressure Drilling. Master's thesis, Norwegian University of Science and Technology, Trondheim.

[9] Egeland, O. and Gravdahl, J. T. (2002). *Modeling and Simulation for Automatic Control*. Marine Cybernetics, Trondheim, Norway.

[10] Gjengseth, C. and Svenum, T. (2011). Heave Compensated Managed Pressure Drilling: A Lab Scaled Rig Design. Project thesis, Norwegian University of Science and Technology, Trondheim.

[11] Gleditsch, M. S. (2013). Disturbance Attenuation in Managed Pressure Drilling Using Impedance Matching and an Experimental Lab Setup. Master's thesis, Norwegian University of Science and Technology, Trondheim.

[12] Godhavn, J. M. (2010). Control Requirements for Automatic Managed Pressure Drilling System. *SPE Drilling & Completion*, 25(3):336 – 345.

[13] Hannegan, D. M. (2005). Managed Pressure Drilling in Marine Environments - Case Studies. *SPE/IADC Drilling Conference, 23-25 February, Amsterdam, Netherlands*.

[14] Kaasa, G., Stamnes, O. N., Imsland, L., and Aamo, O. M. (2011). Intelligent Estimation of Downhole Pressure Using a Simple Hydraulic Model. *IADC/SPE Managed Pressure Drilling and Underbalanced Operations Conference and Exhibition, 5-6 April, Denver, Colorado, USA*.

[15] Landet, I. S., Mahdianfar, H., Aarsnes, U. J. F., Pavlov, A., and Aamo, O. M. (2012a). Modeling for MPD Operations with Experimental Validation. *IADC/SPE Drilling Conference and Exhibition, 6-8 March, San Diego, California, USA*.

[16] Landet, I. S., Pavlov, A., Aamo, O. M., and Mahdianfar, H. (2012b). Control of Heave-Induced Pressure Fluctuations in Managed Pressure Drilling. *American Control Conference 27-29 June, Montreal, QC, Canada*, pages 2270–2275.

[17] Mäkinen, J., Piché, R., and Ellman, A. (2000). Fluid Transmission Line Modeling Using a Variational Method. *Journal of Dynamic Systems, Measurement, and Control*, 122(1):153–162.

[18] McAndrews, K. L. (2011). Consequences of Macondo: A Summary of Recently Proposed and Enacted Changes to US Offshore Drilling Safety and Environmental Regulation. *SPE Americas E&P Health, Safety, Security, and Environmental Conference, 21-23 March, Houston, Texas, USA*.

[19] Møgster, J., M., G. J., and Imsland, L. (2013). Using MPC for Managed Pressure Drilling. *Modeling, Identification and Control*, 34(3):131 – 138.

[20] Nas, S. W. and Toralde, J. S. (2009). Offshore Managed Pressure Drilling Experiences in Asia Pacific. *SPE/IADC Drilling Conference and Exhibition, 17-19 March, Amsterdam, The Netherlands*.

[21] Rehm, B., Schubert, J., Haghshenas, A., Paknejad, A. S., and Hughes, J. (2008). *Managed Pressure Drilling*. Gulf Publishing Company, Huston, USA.

[22] Skogestad, S. and Postletwaite, I. (2007). *Multivariable Feedback Control Analysis and Design*. John Wiley & Sons Ltd, Chichester, England, 2 edition.

[23] Stecki, J. S. and Davis, D. C. (1986a). Fluid Transmission Lines – Distributed Parameter Models Part 1: A Review of the State of the Art. 200(4):215–228.

[24] Stecki, J. S. and Davis, D. C. (1986b). Fluid Transmission Lines – Distributed Parameter Models Part 2: Comparison of Models. 200(4):229–236.

[25] Totland, J. F. H. (2013). Modeling of Transients in Drilling for Controller Design. Project thesis, Norwegian University of Science and Technology, Trondheim.

[26] Watton, J. and Tadmori, M. J. (1988). A Comparison of Techniques for the Analysis of Transmission Line Dynamics in Electrohydraulic Control Systems. *Applied Mathematical Modelling*, 12(5):457 – 466.